PH004

Growth Analysis of the Sunspot in AR12741 using High-Resolution Solar Imaging

Report

1. Introduction

a. Background

The modern world relies heavily on electricity and technology to function, and they have become an important part of our lives. The sun is our primary source of energy and the reason life exists on the Earth, however the phenomena occurring on it could be devastating to the very technology this world needs. Thus it is necessary for us to understand its complex working in depth. Solar astronomy is becoming more and more accessible to individuals around the world who can observe the sun almost as well as the space agencies and make beneficial contributions. Many research projects are ongoing to understand our star[11][16] and through this project, we wish to give some useful contributions on how certain Solar phenomena develop.

b. Aim

The aim of our research is to analyse AR12741 in order to understand the changes during the growth of an active region.

c. Hypothesis

AR12741 will increase in activity after its formation, to a point where its activity is maximum, and will then decrease in its activity, eventually vanishing from the surface of the sun.

2. Methodology

The experiment had four major components, namely experimental setup, data collection, data processing and image scaling. They are discussed in depth below.

a. Experimental Setup *(Check Appendix A for setup image)*

The setup used comprises of:

1. 220mm Dielectric Energy-Rejection Filter
2. Celestron C8-A-XLT Schmidt Cassegrain Telescope

3. H-Alpha single etalon filter with 0.9 Å bandwidth around 656.28 nm
4. Basler acA1920-40 μm [4]
5. x2 Barlow
6. iEQ 60 Center-balanced Equatorial Mount [5]

For high resolution imaging, it is crucial for the mount to track the sun accurately as even a slight inaccuracy would cause a substantial drift in the high-resolution video. Thus, the mount was aligned as follows:

1) The mount was polar aligned using a compass by pointing its polar axis to the magnetic north pole.
2) To ensure good tracking without the need of autoguiding, drift alignment was carried out using procedure by Clay Sherrod[6].

Then the tracking accuracy was tested by pointing the scope at different stars and ensuring that the drift is not more than 1 arcsec/min.

b. Data Collection *(check the Appendix B for related images)*

The data was collected using FireCapture software. First the C8 was pointed at the active region. The gain and exposure were set to minimise the problems caused by Earth's turbulent atmosphere. From trials, it was established that exposures of 2 to 2.5ms with a medium gain is essential for high resolution imaging, short enough to freeze the seeing and quick enough to get a good frame per second speed. Then the image was focused and the video was shot. The shot lasted 30-45 sec to record about 2000 frames while ensuring the drift was not more of 3 pixels/min. After the main video was shot, the scope was defocused completely without changing the gain and exposure values and a short flat video was shot to remove the noise from the image later during post-processing.

c. Data Post-Processing *(check Appendix B for related images)*

1. *Autostakkert!*

   The recorded video was then processed in Autostakkert! First, a master flat frame was made by clicking on the "1) Open" button and choosing the recorded flat video. Then

from the Image Calibration menu, a master flat was created which was subtracted from the recorded video using the image calibration menu again. The video frames recorded in the most favorable atmospheric conditions[8] were carefully selected using the frame-quality curve. Frames of at least 90% quality were selected and stacked as an unsharpened .tif file which was later put through an image reconstruction processing[12].

2. *Adobe Photoshop*

   The stacked files were cropped in photoshop, to remove any stacking artifact. It is important to remove them as they can drastically change the histogram of our image, causing problems during curve stretching later on.

3. *ImPPG*

   At the start of the image reconstruction process, the cropped files were then post processed in the free open-source software ImPPG. As previously mentioned, the cloud cover was much lighter on 14th May than 11th May and thus, the images have considerably different noises. Hence the parameters used in their processing vary. First, the tone curve was stretched to increase the contrast of the image. Another node was selected before the stretched node and was lowered to achieve a clear contrast between the sunspot, facula and the filament in the active region. The stretched tone curve also makes it much easier to observe the effects of Lucy-Richardson deconvolution[15]. This was followed by adjusting the LR deconvolution to sharpen the image. The sigma was first increased to a high value, and then brought down to the point where the details in the image were enhanced, but not bloated. Further precise sharpening was performed through adaptive unsharp masking. Minimum amount and the threshold were set to their respective highest values, 100 and 1. The maximum amount was kept at 0. This was done to accurately select the regions that will be sharpened by the minimum and the maximum amount. The maximum amount sharpens the brighter region of the image and thus the threshold was reduced such that only the facula was not affected. The transition width was then adjusted to ensure a smooth sharpening effect between the regions affected by minimum and maximum amount. At last, the sigma was adjusted. The image was zoomed near the sunspot and sigma value was changed. The final sigma value was such that it did

not bloat the fibrils but at the same time made two adjacent fibrils easily differentiable. This is analogous to a quadratic curve with a minimum point. Then the images were saved as .tif files.

4. *Image scaling*

Using the formula[3],

$$\text{Computational formula of image scale} = \left(\frac{\text{pixel size of camera}}{\text{focal length of optical system}}\right) \times 206.265$$
$$= \left(\frac{5.86}{2032 \times 2}\right) \times 206.265$$
$$= 0.2977 \ arcsec/pixel$$

The image scale was found to be approximately 0.3 arcsec/pixel. This was later used during data analysis.

3. Results

The final processed images of AR12741 on 11th May, 14th May and 15th May are shown below with the corresponding full disk images taken from SDO[1].

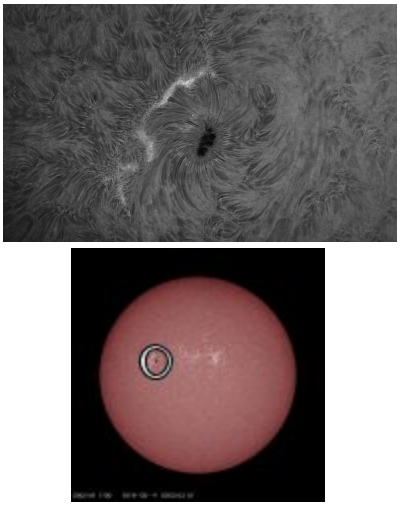

Figure 1. Processed image of AR12741 on 11th May and corresponding full disk image from SDO

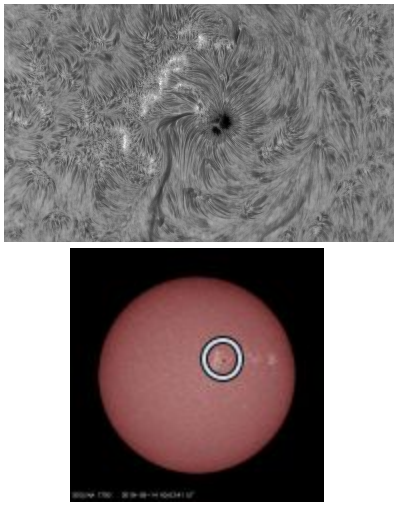

Figure 2. Processed image of AR12741 on 14th May and corresponding full disk image from SDO

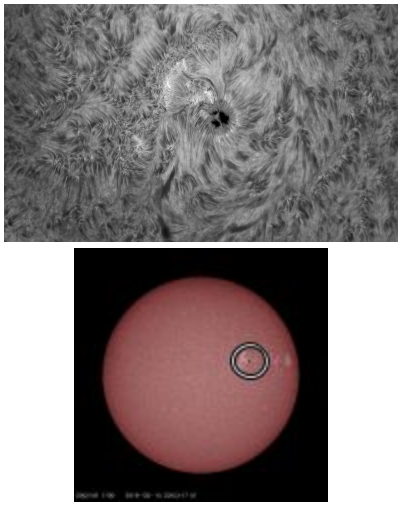

Figure 3. Processed image of AR12741 on 15th May and corresponding full disk image from SDO

To better understand the filament most visible on 14th May, images surrounding the complete filament were captured as well

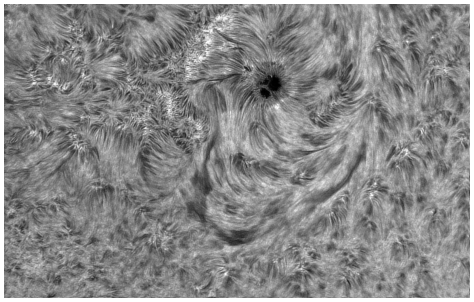

Figure 4. Image of the area below the filament on 14th May

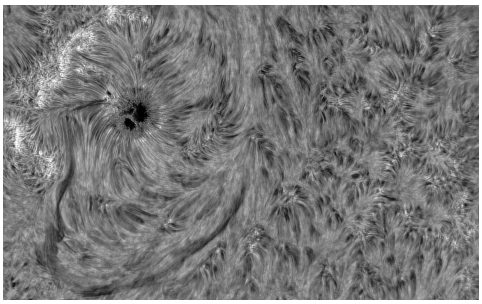

Figure 5. Image of the area to the right of filament on 14th May

Moreover, to further analyse the growth of the sunspot, data for 16th May obtained from Solar Chat Forum[9] was used to check the observed trend.

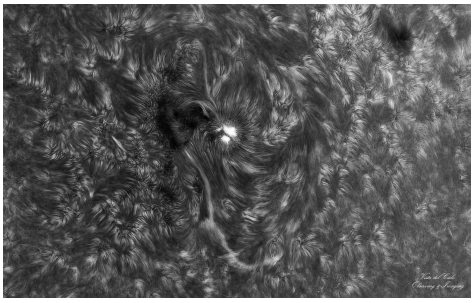

Figure 6. Image of AR12741 on the 16th of May, obtained from a user on Solar Chat Forum.

4. Discussion and Analysis

a. Magnetic Field of the Sun

There are millions of magnetic poles on the sun. The constant interaction of these magnetic fields result in the different solar features and activities which are visible in the images above[7]. It can be observed in Figures 1 to 6 that the region away from the sunspot has a very chaotic plasma flow. This is because the sun is not a solid sphere, but rather a ball of gas and undergoes differential rotation. Thus the magnetic field intercepts giving rise to a rather complex net magnetic field. In order to visualise the non-uniform magnetic field, HMI Magnetogram was used and can be found in Appendix C. The black regions have south magnetic polarity, while the white regions have north polarity[14]. Based on the magnetograms, it can be concluded that the sun indeed has a complex magnetic field. Since plasma follows the magnetic field, this results in a chaotic plasma flow as observed in our images. There are many on-going studies to understand and predict solar activities[11]. Our observation on the evolution of AR127431 affirmed the

unpredictable nature and dynamic changes in the magnetic fields which were observed in the solar features.

b. Sunspot

Sunspots are darker regions on the sun through which magnetic field lines of the sun penetrate out of the sun's surface, reducing its temperature which makes it appear dark against the bright background[7]. The growth of sunspots was measured using the *Sunspot Measurement Program* (SMP) developed by us (refer to Appendix D for the detailed working of the program) along with visual observations and data from other observatories. On 11th May, the area of the sunspot was 4.47×10^9 square kilometres, which decreased to 1.42×10^9 square kilometres on 14th May and then to 9.36×10^8 square kilometres on 15th May. Data recorded by US National Oceanic and Atmospheric Administration's (NOAA) GOES14 system showed that AR12741 produced several B-Class minor flares and C-Class flares between 12 and 15 May[13]. These flares caused the sunspot to expend part of its energy and it started to reduce in size. Our images also helped us identify another reason for the decay of the sunspot - the formation of light bridges. They are loosely defined as any material brighter than an umbra that also divides the umbra, sometimes even dividing the penumbra[7]. On 11th May, the first light bridge can be seen extending into the southeast section of the umbra. The light bridge extends further and divides the umbra into two segments by 14th May, and a second light bridge begins dividing the upper umbral segment from the north. By 15th and 16th May, the second light bridge completely divides the umbra into three distinct segments, thus decreasing the overall area. The sunspot is unipolar which can be seen in the magnetogram in Appendix C. Moreover, it has a well defined elliptically shaped penumbra. Thus, it was classified as Hsx using McIntosh Sunspot classification[2][10]. The sunspot also shows the Wilson effect, as its shape changes from being elongated to rather circular as it moves from the limb to the central disk, as observed in figures 1 to 3 and 6[7].

c. Filament

Filaments are large regions of cool, dense gas suspended above the Sun's surface by magnetic fields[7]. A filament can be seen clearly on 14th and 15th May as seen in figure 2 and 4 to 6. There was an increase in the size and length of the filament on the 15th of May, and the filament

appeared to have separated from the main sunspot on 15th May. We conjecture the change in its shape and location is due to the changing magnetic field of the sun, as discussed earlier.

d. Facula

Facula are bright and hot spots in the surface of the Sun with strong magnetic fields (but comparatively weaker than sunspots) in the pattern of convective cells[7]. In figures 1 to 3, the facula appears lighter in colour relative to the sunspot and the surrounding plasma. From 11th to 15th May, a faculae to the left of the sunspot can be seen diminishing in brightness and size across the days, and almost vanishing altogether on the 15th. This is because of the fact that a facula is the precursor to a sunspot. As the sunspot develops further, the facula eventually disintegrates.

5. Future Works

Using knowledge gained from this research, we can use our understanding of data capturing and image processing and apply it to observe other solar phenomena like filaments, prominences, and coronal mass ejections. These phenomena will provide insight into how filaments form and eventually disappear, as well as how filaments can lead to coronal mass ejections. SMP could be improved further by increasing its sensitivity for sunspot regions, as well as by considering the curvature of the sun in area calculation.

6. Conclusion

In conclusion, AR12741 gave us insight on the development of sunspot, filament as well as facula. The sunspot developed, decreasing in size as days passed by due to the formation of light bridges and ejection of B-Class and C-Class flares. The filament became visible on 14th May and then it eventually broke off from the main sunspot region. The facula was visible from the starting, but it disintegrated as time passed by. The main factor behind all these observations is the dynamic magnetic field of the sun. While this singular observation seems to suggest that the hypothesis is true, much more data and observations are required to completely prove it. We believe in the future, the findings in this research could be applied to other active region formations as well. Also, the program used to measure sunspot development will be developed further, so that it becomes a valuable asset in solar astronomy.

6. References

1. *Addison, K. (2021). SDO* | Solar Dynamics Observatory. *Retrieved from* https://sdo.gsfc.nasa.gov/data/
2. *AR12741 History*. (n.d.). https://helio-vo.eu/solar_activity/arstats/arstats_page4.php?region=12741
3. *astronomy.tools*. Astronomy.tools. (2021). Retrieved 1 January 2021, from https://astronomy.tools/calculators/ccd.
4. *Basler acA1920-40um, 1/1.2 in. format, C-Mount, 1920 x 1200, 40 fps, Monochrome, CMOS Global Shutter, USB3 Vision - Graftek Imaging Inc*. (n.d.). Retrieved January 19, 2021, from https://graftek.biz/products/basler-aca1920-40um-1-slash-1-dot-2-in-dot-format-c-mount-1920-x-1200-40-fps-monochrome-cmos-global-shutter-usb-3-dot-0
5. *CEM60*. (n.d.). Retrieved January 19, 2021, from https://www.ioptron.com/product-p/7200.htm
6. Clay, D. (n.d.). *Arkansas Sky Observatories - Drift Method for Precise Polar Alignment*. http://arksky.org/aso-guides/aso-telescope-performance/108-drift-method-for-precise-polar-alignment
7. Jenkins, J. L.(2013). *Observing the Sun: A Pocket Field Guide*. Springer.
8. Law, N., Mackay, C., & Baldwin, J. (2006). Lucky imaging: high angular resolution imaging in the visible from the ground. *Astronomy & Astrophysics*, *446*(2), 739-745. https://doi.org/10.1051/0004-6361:20053695
9. M. (2019, May 16). *Close to AR2741 ... Quark Prominence ... UPDATE - SolarChat!* https://solarchatforum.com/viewtopic.php?f=4&t=26136
10. McIntosh, P. S. (1990). The classification of sunspot groups. *Solar Physics*, *125*(2), 251–267. https://doi.org/10.1007/bf00158405

11. *Parker Solar Probe: The Mission*. Parkersolarprobe.jhuapl.edu. (2021). Retrieved from http://parkersolarprobe.jhuapl.edu/The-Mission/index.php.
12. Popowicz, A., Radlak, K., Bernacki, K., & Orlov, V. (2017). Review of Image Quality Measures for Solar Imaging. *Solar Physics*, *292*(12). https://doi.org/10.1007/s11207-017-1211-3
13. *Sun flares*. Tesis.lebedev.ru. (2021). Retrieved from https://tesis.lebedev.ru/en/sun_flares.html?m=5&d=16&y=2019.
14. Svs, N. (n.d.). *SVS: The Active Sun from SDO: HMI Magnetogram*. https://svs.gsfc.nasa.gov/3989
15. Szczerek, F. (n.d.). *ImPPG Processing Tutorial*. www.Greatattractor.Github.Io. https://greatattractor.github.io/imppg/tutorial/tutorial_en.html
16. Tan, A. (2020). High-resolution solar imaging for citizen science. *EPJ Web of Conferences*, *240*, 1–4. https://doi.org/10.1051/epjconf/202024001002

Appendix A: Setup

Figure 7: Setup used for imaging

Appendix B: Softwares

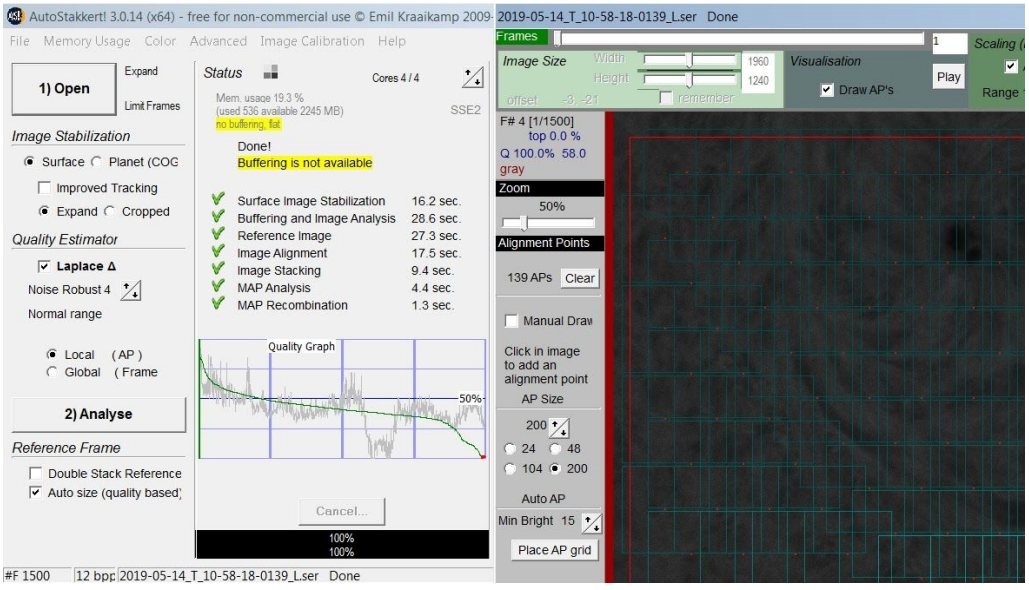

Figure 8: Autostakkert user interface

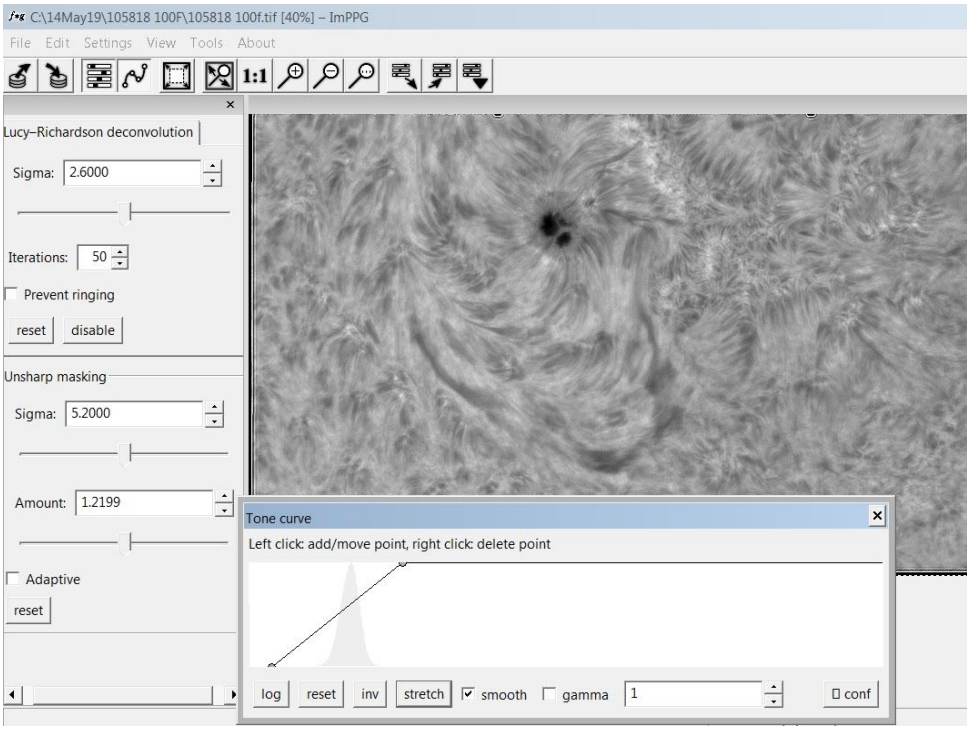

Figure 9: imPPG user interface

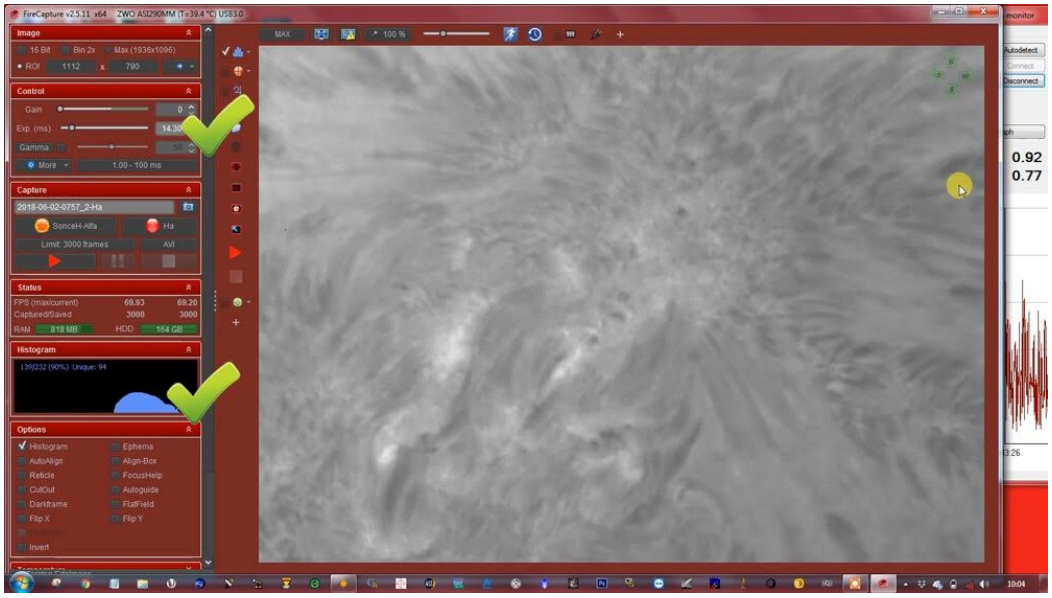

Figure 10: FireCapture user interface

Appendix C: HMI Magnetogram Images

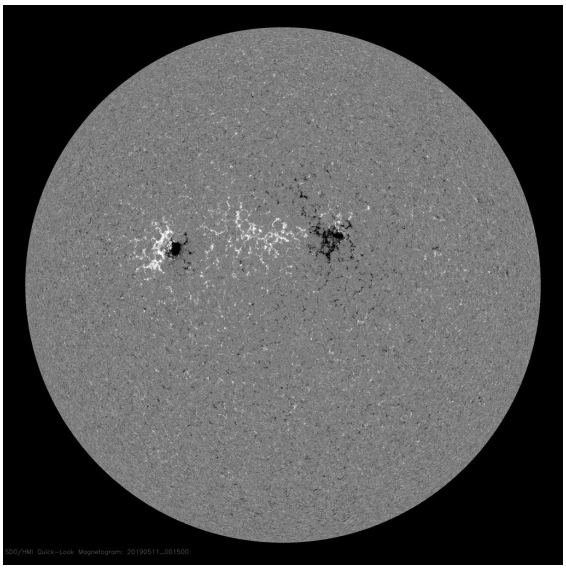

Figure 11: 11 May

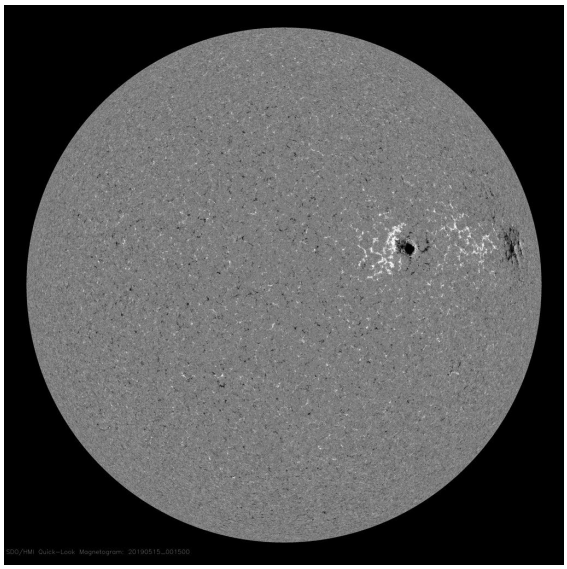

Figure 12: 14 May

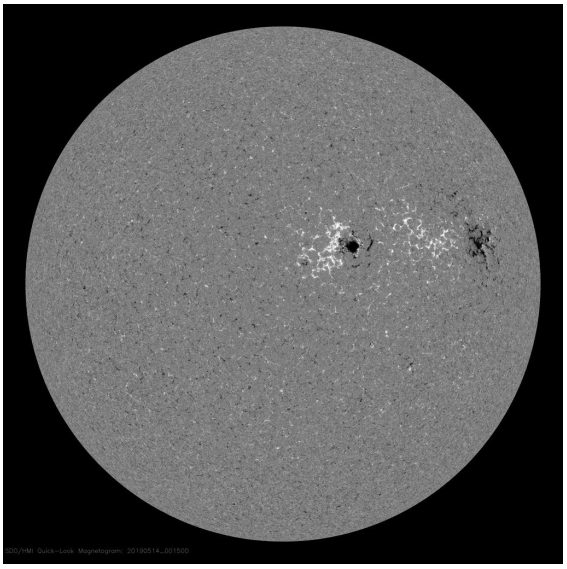

Figure 13: 15 May

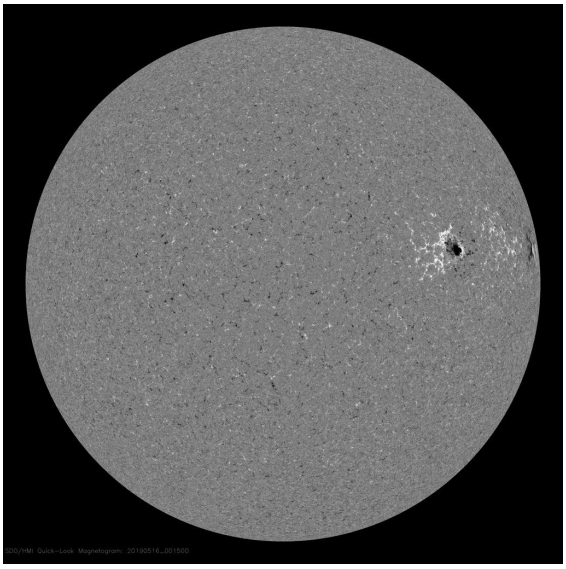

Figure 14: 16 May

Appendix D: Sunspot measurement program

The program was written in Python using tkinter GUI. The program inputs an image and calculates the average RGB value of the pixels in the image. Using that, we can then choose a threshold value. Then, it forms contour on the image and calculates the area inside it. The output is the number of pixels in the contour area. The threshold value is used to determine the contour edges. All the pixels above the contour value is coloured white, while everything below is coloured black. Using the number of pixels and the image scale, the area covered by the sunspot is calculated. The figures below show the output of the code.

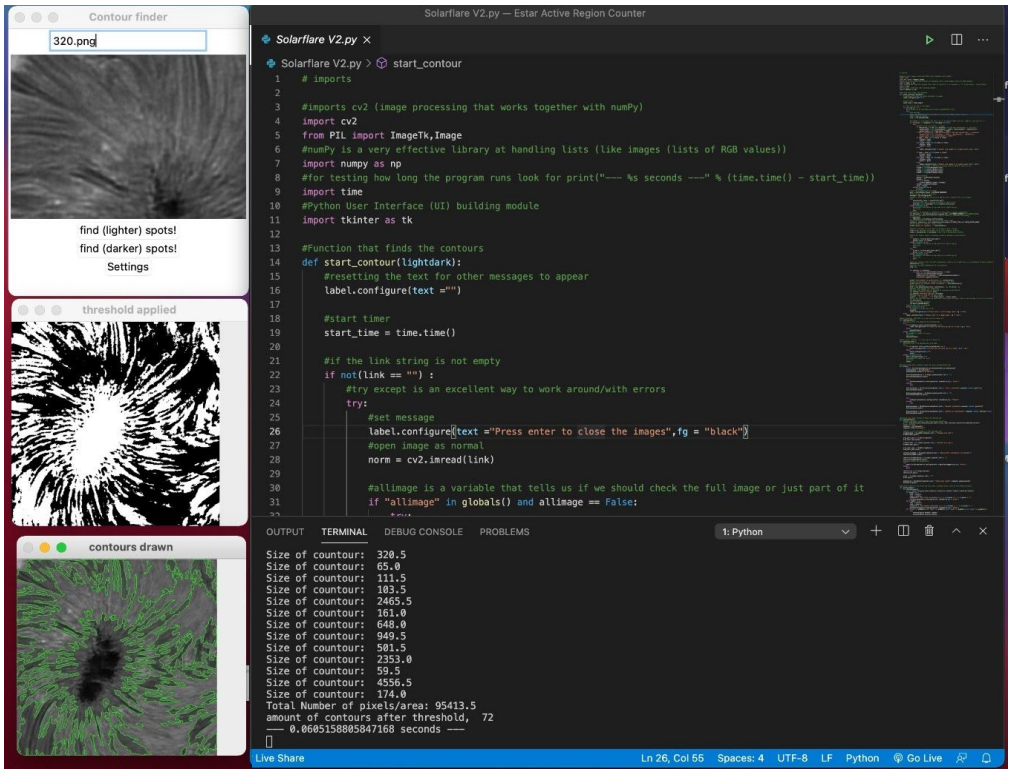

Figure 15: Output for 11th May

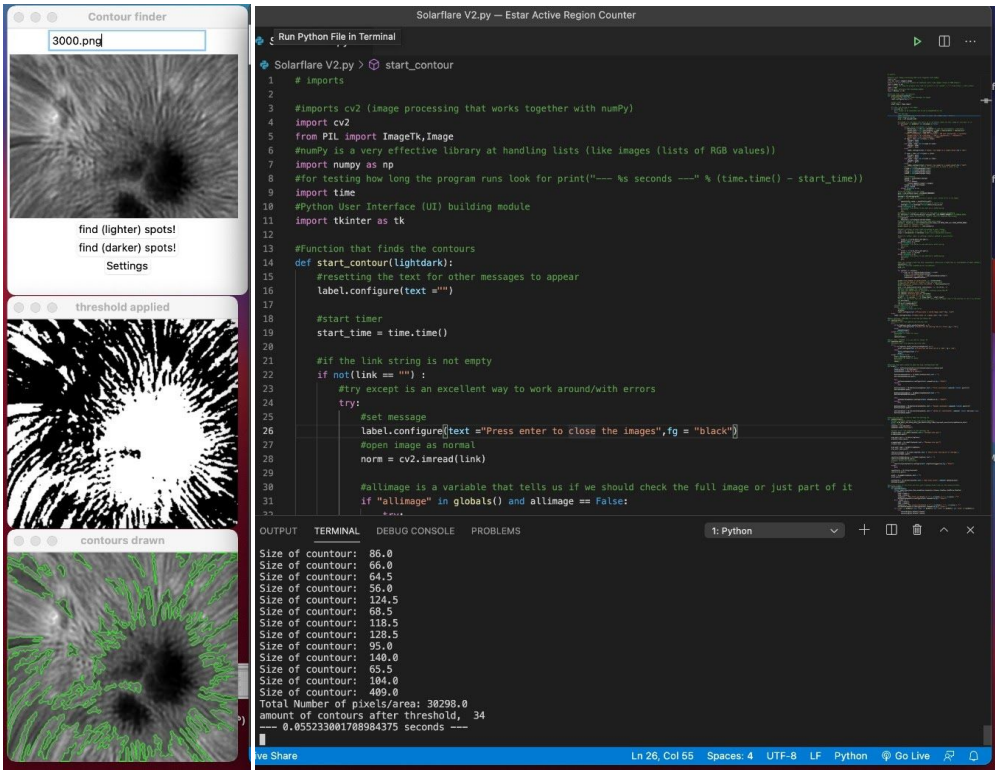

Figure 16: Output for 14th May

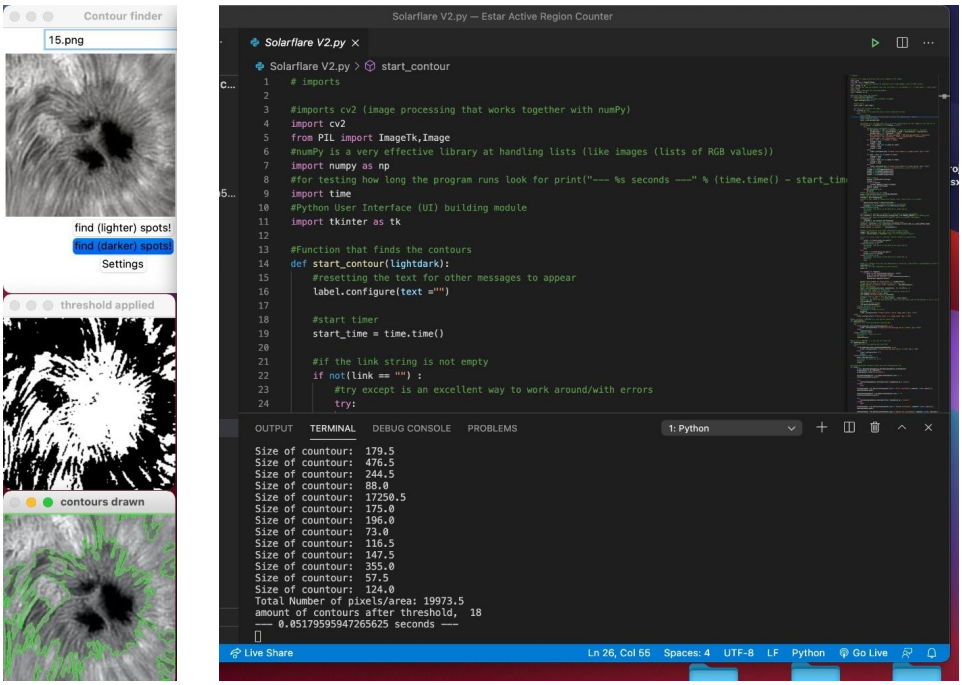

Figure 17: Output for 15th May